ELSEVIER

Journal of Photochemistry and Photobiology A: Chemistry 146 (2001) 95–107

Journal of Photochemistry and Photobiology A:Chemistry

www.elsevier.com/locate/jphotochem

Fluorescence properties of phenolate anions of coelenteramide analogues: the light-emitter structure in aequorin bioluminescence

Yuko Imai [a], Takuya Shibata [a], Shojiro Maki [a], Haruki Niwa [a], Mamoru Ohashi [b], Takashi Hirano [a,*]

[a] *Department of Applied Physics and Chemistry, The University of Electro-Communications, Chofu, Tokyo 182-8585, Japan*
[b] *Department of Materials Science, Kanagawa University, Hiratsuka, Kanagawa 259-1293, Japan*

Received 26 April 2001; received in revised form 17 July 2001; accepted 30 July 2001

Abstract

To elucidate the ionic structure of the excited state of light-emitter coelenteramide in aequorin bioluminescence, the fluorescent properties of phenolate anions of coelenteramide analogues were investigated. Fluorescence of phenolate anion in non-polar solvents was observed by electronic excitation of a 1:1 hydrogen-bonded complex of a coelenteramide analogue with a hydrogen-bond donor molecule such as *n*-butylamine. In polar solvents, the phenolate anion was directly generated using a base, and its fluorescence was studied. These results confirm that the singlet-excited state of phenolate anion of coelenteramide has an intramolecular CT character, and that its fluorescence emission wavelength changes depending upon solvent polarity. The fluoro-substituent effect on the fluorescent property of phenolate anions was also clarified to help in explaining the bioluminescent property of fluorinated semi-synthetic aequorin. These results consistently support the assignment that the phenolate anion is the ionic structure of the excited light-emitter in BFP during AQ bioluminescence.

Keywords: Bioluminescence; Aequorin; Fluorescence; Solvent effect; Phenolate anion; Intramolecular charge transfer; Hydrogen-bonded complex; Coelenteramide

1. Introduction

The calcium activated photoprotein aequorin (AQ) is the bioluminescent substrate of the jellyfish *Aequorea aequorea*, and belongs to a category of calcium-binding proteins with EF-hand structures. When AQ chelates calcium ions, a bioluminescence reaction is initiated which yields an excited singlet state of a blue fluorescent protein (BFP) emitting blue light (Scheme 1) [1–3]. Therefore, AQ has been used as a calcium ion-indicator in the field of biological imaging [4]. From the viewpoint of modern chemistry, AQ is a supramolecule made up of apoaequorin (apoprotein, apoAQ), a luminescent substrate coelenterazine (**1**), and molecular oxygen. In the year 2000, the crystal structure of AQ was revealed at 2.3 Å resolution by Head et al. [5]. In the supramolecular structure of AQ, **1** is in the peroxide (oxygenated) form surrounded by hydrophobic side-chains of amino acid residues at the active site of apoAQ. On the basis of the crystal structure of AQ, we are now in a position to study the molecular process of AQ bioluminescence.

The molecular process of the AQ bioluminescence reaction is based on an oxidation reaction of coelenterazine **1** with O_2, which yields an excited state of coelenteramide (**2**) and CO_2. The singlet-excited state of **2** is the light-emitting species in BFP and emits blue light with an emission maximum at 465–470 nm [6]. One fundamental problem unsolved in the reaction mechanism is elucidation of the ionic structure of excited coelenteramide (**2**) in BFP. Coelenteramide **2** has three dissociable acidic protons located at two phenolic hydroxy groups and an amide moiety. Deprotonation of the 4-hydroxyphenyl group at C5 or of the N–H of amide moiety in the π-conjugated system affects emission wavelength. The hydroxy group of the 4-hydroxyphenylacetamide moiety is not an essential part of **2** for determining the bioluminescence emission wavelength, because a semi-synthetic aequorin which contains coelenterazine analogue possessing a phenylmethyl group at C2 shows the same emission maximum as that of wild type AQ [7,8]. Thus, phenolate anion **I** or amide anion **II** are the possible ionic structures for the excited state of **2** in BFP (Scheme 2). The participation of an excited anion species in AQ bioluminescence was supported by the evidence that bioluminescence of a semi-synthetic aequorin

* Corresponding author. Tel./fax: +81-424-86-1966.
E-mail address: hirano@pc.uec.ac.jp (T. Hirano).

1010-6030/01/$ – see front matter
PII: S1010-6030(01)00554-8

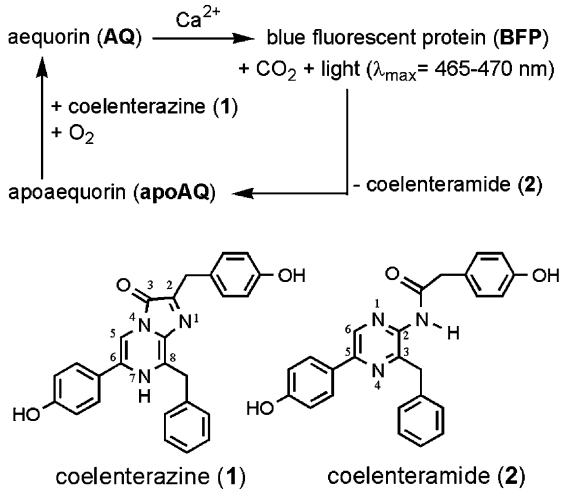

Scheme 1.

(e-AQ) [9,10] and a tryptophan-modified aequorin mutant (AQW86F) [8] showed two-peak emission spectra with emission maxima at 465–470 and 400 nm. The 465–470 nm peak is assigned to emission from the excited anion species and the 400 nm peak is assigned to emission from the excited neutral species **III** (unionized form, Scheme 2).

On the basis of the results of chemiluminescence reactivity of coelenterazine derivatives [11,12], the amide anion **II** has been believed by many researchers to be the excited anion species in AQ bioluminescence. Coelenterazine (**1**) reacts with O_2 in an aprotic solvent, such as dimethylsulfoxide (DMSO) followed by blue light emission with emission maximum around 470 nm. The structure of the excited light-emitter in chemiluminescence is the same as the amide anion **II** of coelenteramide **2**. This similarity has been the main reason to support the assignment to **II**.

The assignment to phenolate anion **I** as the ionic structure of the excited coelenteramide **2** in AQ bioluminescence has been proposed on the basis of several reasons. First, we noted the stability of BFP and the acidity of the phenolic hydroxy group of **2**. A spent solution obtained after a bioluminescence reaction of AQ contains BFP, and this BFP is stable at ambient temperature. The fact that the fluorescence spectrum of the obtained BFP matches the bioluminescence spectrum of AQ [6,13] suggests that the ionic structure of **2** in excited BFP is the same as that in AQ bioluminescence. The acidity of the phenolic hydroxy groups is stronger than that of amide NH in the ground state [14], and phenolic hydroxy groups in the singlet-excited state are more acidic than those in the ground state [15]. Thus, we have supposed that the phenolate anion **I** is the ionic structure of **2** in excited BFP [16]. As other evidence, semi-synthetic BFPs were prepared by incubation of coelenteramide analogues possessing an *N*-methyl group at the amide moiety with apoAQ, and they showed the fluorescence around 480 nm [16]. This result suggests that it is not essential in reproducing the spectrum of AQ bioluminescence to deprotonate the N–H of the amide moiety. Furthermore, we were able to observe fluorescence of a phenolate anion by electronic excitation of a hydrogen-bonded complex of a coelenteramide derivative with an amine in non-polar solvent benzene [17]. Fluorescence of the phenolate anion **I** of **2** had the same emission maximum as seen in AQ bioluminescence. We also used this method to investigate the bioluminescence of fluorinated semi-synthetic AQs [17]. To slightly modify the bioluminescence of AQ, fluorinated coelenterazine analogues **3a**,**b** were used to prepare semi-synthetic AQs. One of the remarkable results was a blue-shifted bioluminescence (λ_{max} 440 nm) using **3a**. The fluorescence of the phenolate anion of fluorinated coelenteramide analogue corresponding to **3a** showed the same blue-shifted emission (λ_{max} 440 nm) via a hydrogen-bonded complex. On the other hand, the emission from the excited amide anion generated by chemiluminescence reaction of **3a** showed only a negligible shift [17]. Thus, we strongly propose the assignment to phenolate anion **I** as the ionic structure of excited **2** in AQ bioluminescence.

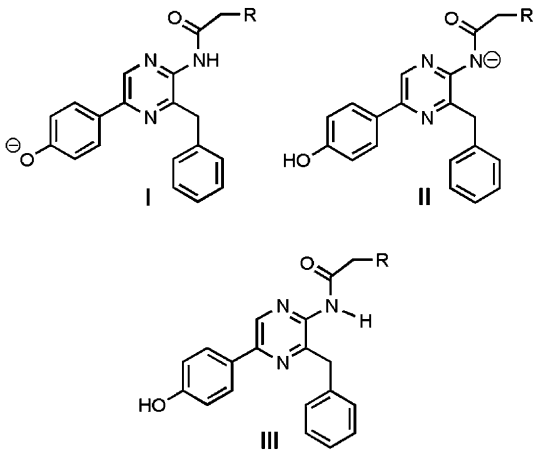

Scheme 2. R = 4-hydroxyphenyl or 4-oxidophenyl.

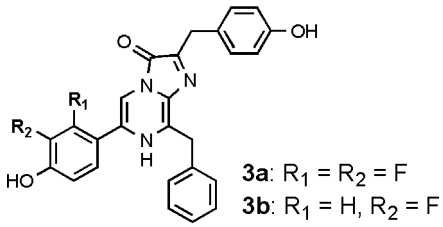

To prove this, it is necessary to systematically investigate the fluorescent properties of coelenteramide derivatives. Although some research on the fluorescence of coelenteramide derivatives has been done [18,19], the properties of coelenteramide derivatives in the excited state have not been systematically characterized. In our previous paper, we confirmed the solvent and substituent effects on the fluorescent property of the neutral form (**III**) of coelenteramide derivatives, and showed that the singlet-excited state of **2** has an intramolecular charge transfer (CT) character with fluorescence shift dependent upon solvent polarity [20].

We have now studied the fluorescent property of phenolate anion **I** systematically. As noted above, we found a condition to observe phenolate anion fluorescence in non-polar solvents by electronic excitation of a hydrogen-bonded complex of a coelenteramide derivative with a hydrogen-bond donor (HBD) molecule. In addition, in polar solvents the fluorescent property of a phenolate anion generated directly using a moderate base was investigated. In this paper, we evaluate the fluorescent properties of phenolate anions of coelenteramide analogues generated under these conditions. For this research, we adopted octanoyl coelenteramide analogues **4**–**6** to improve solubility in various organic solvents. Methoxy analogue **5** was used as a reference compound which did not generate its phenolate anion, and fluorinated analogues **6a**–**c** were used to clarify the reason for the fluoro-substituent effect observed in the bioluminescence of fluorinated semi-synthetic AQs.

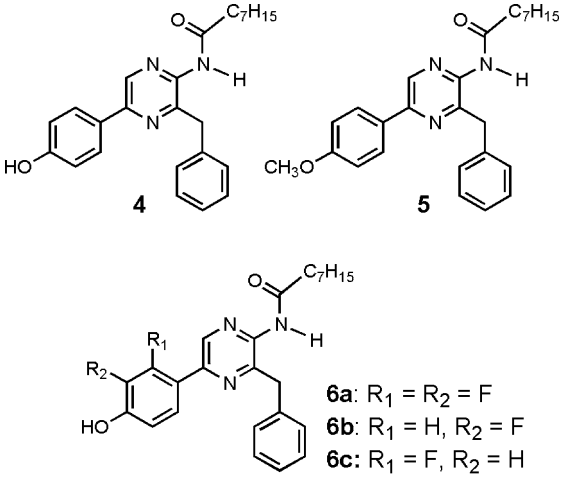

2. Experimental details

2.1. General

^{1}H and ^{13}C NMR spectra were recorded on a JEOL GX-270 instrument (270 and 67.8 MHz, respectively). Melting points were obtained with a Yamato MP-21 apparatus and were used uncorrected. IR spectra were measured with a JASCO IR-810 spectrometer. Electron impact (EI) mass spectra were recorded with a JEOL JMS-600 mass spectrometer. High resolution EI mass spectra were recorded with a JEOL HX-110 mass spectrometer. Elemental analysis was performed by the Instrumental Analyses Center for Chemistry, Graduate School of Science, Tohoku University. UV–Vis absorption spectra were measured with a Varian Cary 50 spectrophotometer or a JASCO V-550 spectrophotometer. Fluorescence spectra were measured with a Hitachi F-4010 fluorescence spectrophotometer (excitation and emission bandpasses, 5 nm; response, 2 s; scan speed, 60 nm/min) and were corrected according to manufacturer's instructions. Fluorescence quantum yields were determined relative to quinine sulfate in 1.0×10^{-4} mol dm^{-3} H_2SO_4 ($\Phi_F = 0.55$, λ_{ex} 355 nm) as the standard. Spectroscopic measurements were made in a quartz cuvette (1 cm path-length) at 25 ± 1°C. Spectral grade solvents were used for measurements of UV–Vis absorption and fluorescence spectra. Semi-empirical MO calculations were carried out with the AM1 Hamiltonian [21] in the MOPAC package (MOPAC2000 ver. 1.0, Fujitsu, Tokyo, Japan, 1999). The geometric structures were fully optimized by the AM1 calculations.

2.2. Synthesis

2.2.1. 3-Benzyl-5-(4-hydroxyphenyl)-2-octanamidopyrazine (**4**)

To a solution of 3-benzyl-5-(4-benzyloxy)phenylpyrazinamine [17] (214 mg, 0.58 mmol) and octanoyl chloride (0.3 ml, 1.8 mmol) in CH_2Cl_2 (7 ml), anhydrous pyridine (1 ml) was added at 0°C, and allowed to warm up to ambient temperature for 1 h. The reaction was quenched by the addition of saturated $NaHCO_3$ aqueous solution, and the product was extracted with $CHCl_3$. The organic layer was washed with brine, dried over Na_2SO_4, and concentrated in vacuo. The residue was purified by silica gel column chromatography ($CHCl_3$/ethyl acetate = 10:1), yielding 3-benzyl-5-(4-benzyloxyphenyl)-2-octanamido-pyrazine (285 mg, 100%) as colorless cubes: ^{1}H NMR (270 MHz, DMSO-d_6) δ 8.88 (s, 1H), 8.03 (m, 2H), 7.31–7.50 (m, 5H), 7.13–7.29 (m, 5H), 7.14 (m, 2H), 5.18 (s, 2H), 4.15 (s, 2H), 2.33 (dd, $J = 6.9$, 7.6 Hz, 2H), 1.52–1.70 (m, 2H), 1.22–1.30 (m, 8H), 0.83–0.86 (m, 3H); IR (KBr) 3276, 3062, 3031, 2927, 2852, 1666, 1608, 1572, 1545, 1496 cm^{-1}; MS (EI, 70 eV) *m/z* (%) 493 (M^+, 100), 229 (59); HRMS (EI) Calcd for $C_{32}H_{35}N_3O_2$ 493.2729, found 493.2736.

To a solution of 3-benzyl-5-(4-benzyloxy)phenyl-2-octanamidopyrazine (49.1 mg, 99 μmol) in a mixture of 1,4-dioxane (15 ml) and ethyl acetate (15 ml), 15 mg of Pd/C powder was added. The suspension was stirred at room temperature for 15 h under H_2, and was filtered through celite. The filtrate was concentrated in vacuo, and the residue was purified by recrystallization, yielding **4** (27.2 mg, 68%) as colorless cubes: mp 190–191°C; ^{1}H NMR (270 MHz, DMSO-d_6) δ 10.20 (br s, 1H), 9.87 (br s, 1H), 8.82 (s, 1H), 7.93 (m, 2H), 7.15–7.29 (m, 5H), 6.87 (m, 2H), 4.13 (s, 2H), 2.32 (dd, $J = 7.2$, 7.3 Hz, 2H), 1.57 (m, 2H), 1.25–1.28 (m, 8H), 0.83–0.88 (m, 3H); IR (KBr) 3289, 2927, 2856, 1670, 1545, 1498 cm^{-1}; MS (EI, 70 eV) *m/z* (%) 403 (M^+, 75), 277 (100), 276 (46), 41 (74); HRMS (EI) Calcd for $C_{25}H_{29}N_3O_2$ 403.2260, found 403.2261.

2.2.2. 3-Benzyl-5-(4-methoxyphenyl)-2-octanamidopyrazine (**5**)

Pyridine (1 ml) was added to a solution of 3-benzyl-5-(4-methoxyphenyl)pyrazinamine [22] (150 mg, 0.52 mmol) and octanyl chloride (0.3 ml, 1.8 mmol) in 5 ml of CH_2Cl_2 at

0°C, and allowed to warm up to ambient temperature for 1 h. The reaction was quenched by the addition of saturated $NaHCO_3$ aqueous solution, and the product was extracted with $CHCl_3$. The organic layer was washed with brine, dried over Na_2SO_4, and concentrated in vacuo. The residue was purified by silica gel column chromatography ($CHCl_3$/ethyl acetate = 10:1) and recrystallization from methanol yielding 3-benzyl-5-(4-methoxyphenyl)-2-octanamidopyrazine (**5**) (140 mg, 65%) as colorless plates: mp 186.5–187°C; ^{1}H NMR (270 MHz, DMSO-d_6) δ 10.11 (br s, 1H) 8.75 (s, 1H), 7.91 (m, 2H), 7.03–7.12 (m, 5H), 6.95 (m, 2H), 4.03 (s, 2H), 3.70 (s, 3H), 2.21 (dd, J = 7.3, 7.4 Hz, 2H), 1.33–1.40 (m, 2H), 1.13–1.20 (m, 8H), 0.74 (m, 3H); ^{13}C NMR (67.8 MHz, DMSO-d_6) δ 172.4 (s), 160.7 (s), 150.6 (s), 148.2 (s), 143.9 (s), 138.4 (s), 137.2 (d), 129.0 (d, 2C), 128.4 (d, 2C), 128.1 (s), 128.0 (d, 2C), 126.4 (d), 114.6 (d, 2C), 55.4 (q), 39.6 (t), 35.5 (t), 31.3 (t), 28.7 (t), 28.5 (t), 25.0 (t), 22.2 (t), 14.1 (q); IR (KBr) 3270, 2952, 2924, 2852, 1664, 1610, 1543, 1496 cm^{-1}; MS (EI, 70 eV) m/z (%) 417 (M^+, 67), 291 (100), 290 (34), 41 (17); Anal. Calcd for $C_{26}H_{31}N_3O_2$: C, 74.79; H, 7.48; N, 10.06, found: C, 74.60; H, 7.11; N, 9.84.

2.2.3. Fluorinated coelenteramide analogues 6a–c

Fluorinated coelenteramide analogues **6a**–**c** were prepared by procedure analogous to that for **4**.

*3-Benzyl-5-(2,3-difluoro-4-hydroxyphenyl)-2-octanamidopyrazine (**6a**)*. Colorless plates: mp 174.5–175°C; ^{1}H NMR (270 MHz, DMSO-d_6) δ 10.12 (br s, 1H), 8.55 (d, J = 2.6 Hz, 1H), 7.43 (ddd, J = 1.6, 8.6, 8.9 Hz, 1H), 7.04–7.17 (m, 5H), 6.81 (ddd, J = 1.6, 8.9, 7.9 Hz, 1H), 4.06 (s, 2H), 2.22 (dd, J = 7.3, 7.3 Hz, 2H), 1.42–1.50 (m, 2H), 1.11–1.21 (m, 8H), 0.72–0.77 (m, 3H); ^{13}C NMR (67.8 MHz, DMSO-d_6) δ 172.1 (s), 150.8 (s), 149.2 (dd, J_{FC} = 12, 250 Hz), 147.9 (dd, J_{FC} = 3.0, 9.2 Hz), 144.3 (s), 144.2 (s), 139.9 (dd, J_{FC} = 15, 233 Hz), 139.7 (dd, J_{FC} = 11 Hz), 138.1 (s), 128.8 (d, 2C), 128.2 (d, 2C), 126.2 (d), 124.2 (ddd, J_{FC} = 3.9, 7.5 Hz), 115.6 (d, J_{FC} = 9.5 Hz), 113.4 (ddd, J_{FC} = 2.2, 4.5 Hz), 39.7 (t), 35.32 (t), 31.1 (t), 28.5 (t), 28.3 (t), 24.8 (t), 22.0 (t), 13.8 (q); IR (KBr) 3275, 2958, 2927, 2854, 1672, 1627, 1541 cm^{-1}; MS (EI, 70 eV) m/z (%) 439 (M^+, 95), 438 (21), 421 (23), 338 (31), 313 (100), 312 (21), 207 (21), 155 (23), 127 (44), 91 (29), 41 (67); HRMS (EI) Calcd for $C_{25}H_{27}F_2N_3O_2$ 439.2071, found 439.2067.

*3-Benzyl-5-(3-fluoro-4-hydroxyphenyl)-2-octanamidopyrazine (**6b**)*. Colorless needles: mp 183–183.5°C; ^{1}H NMR (270 MHz, DMSO-d_6) δ 10.20 (br s, 1H), 8.85 (s, 1H), 7.81 (dd, J = 8.8, 8.9 Hz, 1H), 7.76 (dd, J = 2.0, 8.8 Hz, 1H), 7.15–7.29 (m, 5H), 7.05 (dd, J = 8.8, 8.9 Hz, 1H), 4.14 (s, 2H), 2.33 (t, J = 7.3 Hz, 2H), 1.55–1.60 (m, 2H), 1.22–1.33 (m, 8H), 0.83–0.88 (m, 3H); ^{13}C NMR (67.8 MHz, DMSO-d_6) δ 172.0 (s), 151.3 (d, J_{FC} = 241 Hz), 150.2 (s), 147.1 (d, J_{FC} = 2.2 Hz), 146.4 (d, J_{FC} = 12 Hz), 144.0 (s), 138.2 (s), 137.0 (d), 128.8 (d, 2C), 128.1 (d, 2C), 127.2 (d, J_{FC} = 6.1 Hz), 126.1 (d), 123.0 (dd, J_{FC} = 3.0 Hz), 118.1 (dd, J_{FC} = 3.1 Hz), 114.0 (dd, J_{FC} = 20 Hz), 39.6 (t), 35.3 (t), 31.1 (t), 28.5 (t), 28.3 (t), 24.8 (t), 21.9 (t), 13.8 (q); IR 3276, 2927, 2858, 1672, 1541 (KBr) cm^{-1}; MS (EI, 70 eV) m/z (%) 421 (M^+, 46), 295 (100); HRMS (EI) Calcd for $C_{25}H_{28}FN_3O_2$ 421.2166, found 421.2172.

*3-Benzyl-5-(2-fluoro-4-hydroxyphenyl)-2-octanamidopyrazine (**6c**)*. Colorless plates: mp 182.5–183°C; ^{1}H NMR (270 MHz, DMSO-d_6) δ 10.20 (br s, 1H), 8.59 (d, J = 2.3 Hz, 1H), 7.71 (dd, J = 9.0, 9.2 Hz, 1H), 7.29–7.16 (m, 5H), 6.63 (dd, J = 2.3, 9.0 Hz, 1H), 6.53 (dd, J = 2.3, 14 Hz, 1H), 4.14 (s, 2H), 2.32 (dd, J = 7.3, 7.6 Hz, 2H), 1.57 (m, 2H), 1.18–1.36 (m, 8H), 0.86 (t, J = 6.9 Hz, 3H); ^{13}C NMR (67.8 MHz, DMSO-d_6) δ 172.0 (s), 165.1 (s), 161.3 (d, J_{FC} = 250 Hz), 150.5 (s), 146.1 (s), 142.8 (s), 139.2 (dd, J_{FC} = 13 Hz), 138.3 (s), 130.6 (dd, J_{FC} = 5.9 Hz), 128.8 (d, 2C), 128.1 (d, 2C), 126.1 (d), 113.9 (d), 110.7 (s), 103.1 (dd, J_{FC} = 22 Hz), 39.7 (t), 35.3 (t), 31.1 (t), 28.5 (t), 28.3 (t), 24.8 (t), 21.9 (t), 13.8 (q); IR (KBr) 3292, 3159, 2927, 2854, 1666, 1624, 1496 cm^{-1}; MS (EI, 70 eV) m/z (%) 421 (M^+, 38), 295 (100); HRMS (EI) Calcd for $C_{25}H_{28}FN_3O_2$ 421.2166, found 421.2166.

3. Results and discussion

3.1. Phenolate anion fluorescence of 4 in non-polar solvents

Fluorescence spectral changes of analogue **4** in benzene were observed following the addition of HBD molecules as shown in Fig. 1A. In the presence of *n*-butylamine, tri-*n*-butylamine, or imidazole, a new fluorescence peak with maximum around 470 nm was seen along with decrease of the peak of the neutral form of **4** (λ_{max} 387 nm). Especially, noteworthy was the clear peak at 466 nm observed using *n*-butylamine. The fluorescence behavior of **4** in benzene containing *n*-butylamine matches that of wild-type coelenteramide **2** reported previously [17]. The changes of absorption spectra of **4** in the presence of HBD molecules in benzene were also observed with a small bathochromic shift (Fig. 2A). Fluorescence excitation spectra of **4** in the presence of *n*-butylamine in benzene show that absorption maxima at 331 and 338 nm correspond to emissions at 381 and 466 nm, respectively. In the case of methoxy analogue **5**, its fluorescence and absorption spectra showed only negligible change in the presence of the HBD molecules in benzene (Figs. 1B and 2B), indicating that the spectral change of **4** with an HBD originates from deprotonation of the 4-hydroxyphenyl group in **4**. The large Storks shift (8100 cm^{-1}) of the new fluorescence peak can be explained by generation of a phenolate anion **4**($\mathbf{O}^-$). In the ground state, analogue **4** plus an HBD molecule such as *n*-butylamine form a hydrogen-bonded complex, which reaches equilibrium (Scheme 3). The hydrogen-bonding interaction is too weak to change the electronic properties of **4**, resulting in small changes in absorption spectra.

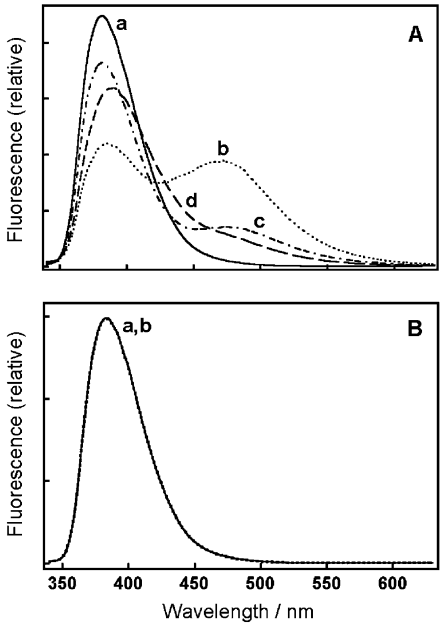

Fig. 1. Fluorescence spectra of **4** (1.5×10^{-6} mol dm^{-3}) (A) and **5** (1.5×10^{-6} mol dm^{-3}) (B) in benzene in the absence and presence of hydrogen-bond donors (0.010 mol dm^{-3}). Hydrogen-bond donor: (a) no hydrogen-bond donor, (b) *n*-butylamine, (c) tri-*n*-butylamine, and (d) imidazole. $\lambda_{ex} = 330$ nm.

Electronic excitation of the hydrogen-bonded complex is followed by deprotonation of the phenolic hydroxy group yielding the excited singlet state of **4**($\mathbf{O}^-$), as expected since the acidity of a phenolic hydroxy group increases in

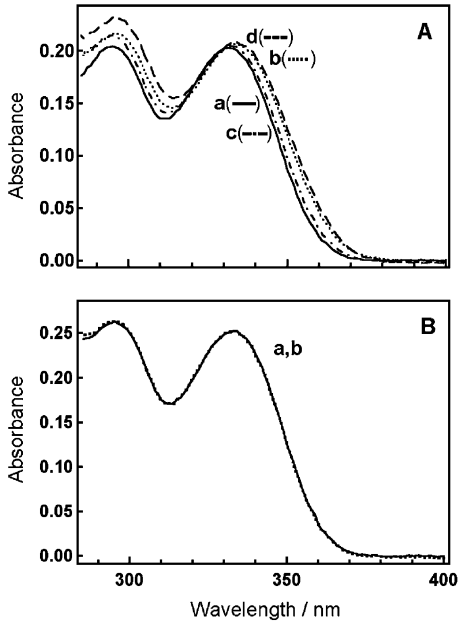

Fig. 2. Absorption spectra of **4** (1.5×10^{-5} mol dm^{-3}) (A) and **5** (1.5×10^{-5} mol dm^{-3}) (B) in benzene in the absence and presence of hydrogen-bond donors (0.010 mol dm^{-3}). Hydrogen-bond donor: (a) no hydrogen-bond donor, (b) *n*-butylamine, (c) tri-*n*-butylamine, and (d) imidazole.

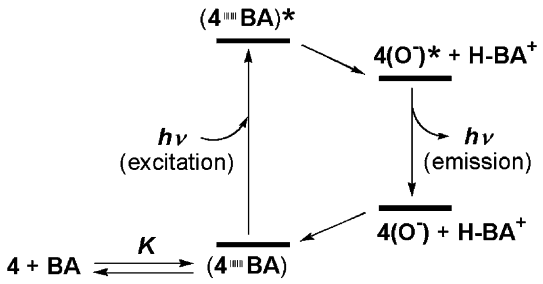

Scheme 3. BA = *n*-butylamine.

singlet-excited states. The singlet-excited state of **4**($\mathbf{O}^-$) emits fluorescence at a longer wavelength (Scheme 3). Similar photochemical processes have been thoroughly studied for the hydrogen-bonded complexes of hydroxyarenes such as naphthol with an HBD molecule [23–25].

To confirm the formation of a hydrogen-bonded complex of **4** and an HBD molecule, a solvent effect on the complex formation was studied quantitatively. In chloroform, the fluorescence spectrum of **4** in the presence of *n*-butylamine also showed a new fluorescence peak (λ_{max} 502 nm) of a phenolate anion **4**($\mathbf{O}^-$) (Fig. 3), although only a shift of fluorescence maximum of **4** itself (neutral form) dependent upon the solvent polarity was observed in DMSO, DMF, and acetonitrile. These results suggest that hydrogen-bonded complexes of **4** with *n*-butylamine are more efficiently formed in non-polar solvents than in polar solvents.

Formation of a 1:1 hydrogen-bonded complex of **4** and *n*-butylamine in benzene was quantitatively evaluated by measuring absorption and fluorescence spectra. Absorption spectra of **4** (λ_{max} 331 nm) in benzene show a slight bathochromic shift of the absorption maximum following the addition of various concentrations of *n*-butylamine to solutions of **4**. Isosbestic points were observed at 330 and 316 nm (Fig. 4A). The equilibrium constant *K* for the formation of the 1:1 hydrogen-bonded complex of **4** with *n*-butylamine is estimated to be 220 ± 30 mol^{-1} dm^3 at 25°C from a double reciprocal plot of these spectral changes (Fig. 4B) [26]. The changes of fluorescence spec-

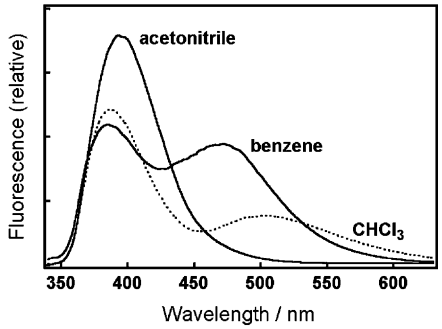

Fig. 3. Fluorescence spectra of **4** (1.5×10^{-6} mol dm^{-3}) in acetonitrile, chloroform, and benzene containing *n*-butylamine (0.010 mol dm^{-3}). $\lambda_{ex} = 330$ nm.

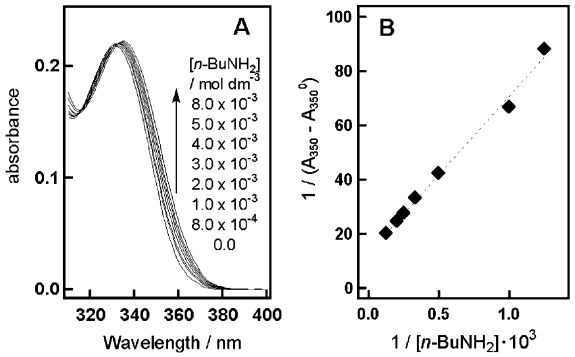

Fig. 4. (A) Absorption spectra of **4** (1.5×10^{-5} mol dm^{-3}) in benzene containing various concentrations of *n*-butylamine (0.0–8.0×10^{-3} mol dm^{-3}) at 25 ± 1°C. (B) Double reciprocal plot of $1/(A_{350} - A_{350}{}^0)$ vs. 1/[*n*-butylamine] for the formation of the hydrogen-bonded complex of **4** with *n*-butylamine.

tra of **4** in benzene containing *n*-butylamine (Fig. 5A) also support the formation of a 1:1 hydrogen-bonded complex of **4** and *n*-butylamine. By excitation at one of the isosbestic point (330 nm), fluorescence spectral changes were observed, and the *K* value for the formation of the 1:1 complex was also estimated as 250 ± 20 mol^{-1} dm^3 (Fig. 5B). This *K* value is similar to the *K* value estimated by absorption spectral measurements. This result suggests that the fluorescence spectral changes by generation of the excited singlet state of **4**(**O**$^-$) reflect the concentration changes of the 1:1 hydrogen-bonded complex reversibly formed in the

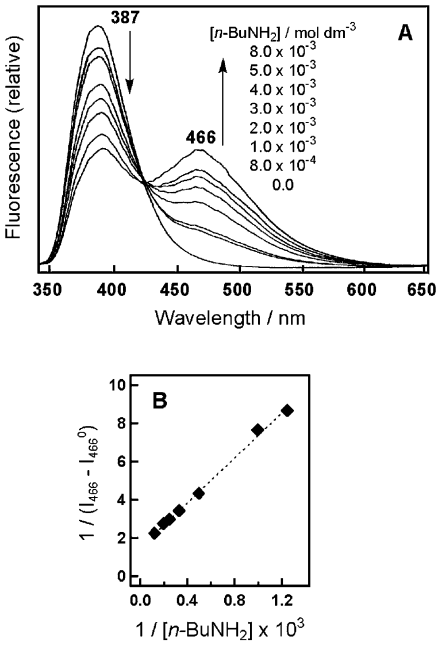

Fig. 5. (A) Fluorescence spectra of **4** (1.5×10^{-6} mol dm^{-3}) in benzene containing various concentrations of *n*-butylamine (0.0–8.0×10^{-3} mol dm^{-3}) at 25 ± 1°C. $\lambda_{ex} = 330$ nm. (B) Double reciprocal plot of $1/(I_{466} - I_{466}{}^0)$ vs. 1/[*n*-butylamine] for the formation of the hydrogen-bonded complex of **4** with *n*-butylamine.

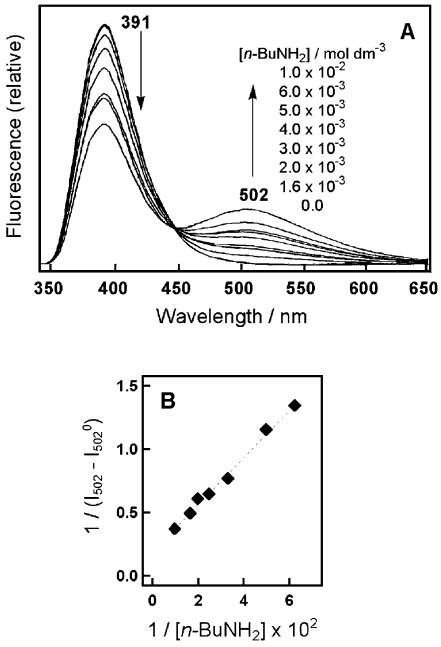

Fig. 6. (A) Fluorescence spectra of **4** (1.5×10^{-6} mol dm^{-3}) in chloroform containing various concentrations of *n*-butylamine (0.0–1.0×10^{-2} mol dm^{-3}) at 25 ± 1°C. $\lambda_{ex} = 330$ nm. (B) Double reciprocal plot of $1/(I_{502} - I_{502}{}^0)$ vs. 1/[*n*-butylamine] for the formation of the hydrogen-bonded complex of **4** with *n*-butylamine.

ground state. The excited singlet state of **4**(**O**$^-$) is mainly generated by electronic excitation of the ground-state complex via deprotonation of the phenolic hydroxy group of **4** in the excited-state complex as shown in Scheme 3. To confirm this mechanism, we need to study a photophysical process of the hydrogen-bonded complex. In chloroform, the equilibrium constant *K* for the 1:1 complex formation was estimated as 100 ± 20 mol^{-1} dm^3 at 25°C by fluorescence spectra alone (Fig. 6), because the absorption spectra showed only small changes in the complex formation. The *K* value for the complex formation in chloroform is smaller than that in benzene. The tendency of a decrease in equilibrium constant *K* with an increase of solvent polarity corresponds to the observation that the hydrogen-bonded complexes of **4** with *n*-butylamine are more efficiently formed in non-polar solvents than in polar solvents. These results are characteristics of hydrogen-bonded complexes [23,24].

When the initial concentration of **4** was 1.5×10^{-6} mol dm^{-3} in benzene containing 4.0×10^{-3} mol dm^{-3} of *n*-butylamine at 25°C, the mole fraction of the 1:1 hydrogen-bonded complex in the total concentration of **4** was calculated as 0.47 using the *K* value 220 mol^{-1} dm^3. Under this condition, the fluorescence spectrum measured by excitation at 330 nm showed two peaks; one from the neutral form of **4** and another from the phenolate anion **4**(**O**$^-$). By subtracting the fluorescence of the neutral form from the total spectrum, the partial peak area of the fluorescence of **4**(**O**$^-$) was obtained. The fluorescence quantum

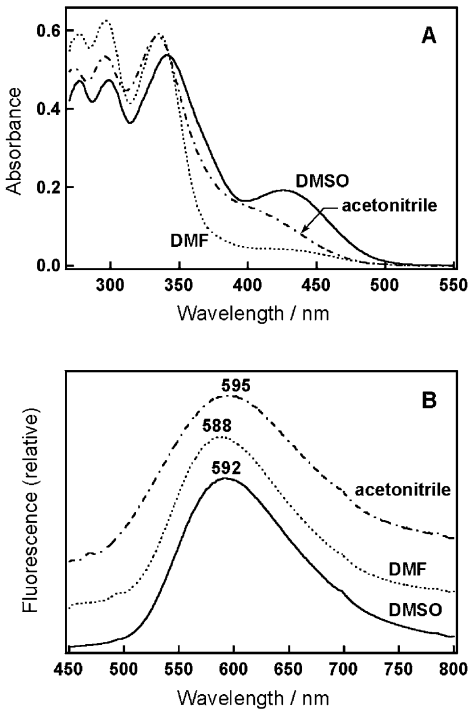

Fig. 7. Absorption spectra (A) and fluorescence spectra (B) of **4** (4.0×10^{-5} mol dm^{-3}) in DMSO, DMF and acetonitrile in the presence of 1,1,3,3-tetramethylguanidine (0.010 mol dm^{-3}). $\lambda_{ex} = 430$ nm in DMSO and DMF, and $\lambda_{ex} = 410$ nm in acetonitrile.

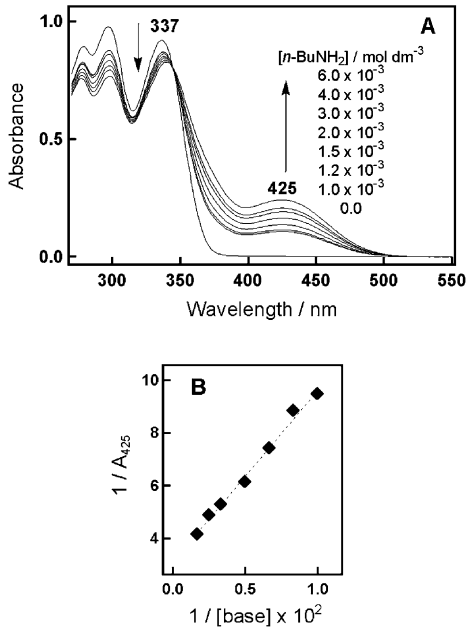

Fig. 8. (A) Absorption spectra of **4** (6.0×10^{-5} mol dm^{-3}) in DMSO containing various concentrations of 1,1,3,3-tetramethylguanidine ($0.0–6.0 \times 10^{-3}$ mol dm^{-3}) at 25 ± 1°C. (B) Double reciprocal plot of $1/A_{425}$ vs. 1/[1,1,3,3-tetramethylguanidine (base)] for the formation of phenolate anion **4**($\mathbf{O}^-$).

yield of **4**($\mathbf{O}^-$) was estimated as 0.23 based on the fluorescence of quinine sulfate as a standard.

3.2. Phenolate anion fluorescence of 4 in polar solvents

In polar solvents, the phenolate anion **4**($\mathbf{O}^-$) was directly generated using a base stronger than *n*-butylamine. For this purpose, an organic base 1,1,3,3-tetramethylguanidine was used in DMSO, DMF, and acetonitrile [27]. Fig. 7A exhibits absorption spectra of **4** in DMSO, DMF, and acetonitrile containing 1,1,3,3-tetramethylguanidine. In the presence of 1,1,3,3-tetramethylguanidine, a new absorption band of a yellow-colored species appeared around 420 nm along with decrease of the peak of the neutral form of **4**. In DMSO, a clear peak was observed at 425 nm. In DMF and acetonitrile, a shoulder was observed around 420 nm. In the case of methoxy analogue **5**, there was no change in absorption spectra in the presence of 1,1,3,3-tetramethylguanidine. These results indicate that the yellow-colored species generated from **4** is the phenolate anion **4**($\mathbf{O}^-$). Fig. 7B illustrates the fluorescence emission spectra of **4**($\mathbf{O}^-$) in DMSO, DMF, and acetonitrile containing 1,1,3,3-tetramethylguanidine. Fluorescence maxima of **4**($\mathbf{O}^-$) were observed at 592, 588, and 595 nm in DMSO, DMF, and acetonitrile, respectively. In DMSO, the Storks shift was calculated as 6600 cm^{-1}. Fluorescence quantum yields were also estimated as 0.016, 0.019, and 0.003 in DMSO, DMF, and acetonitrile, respectively.

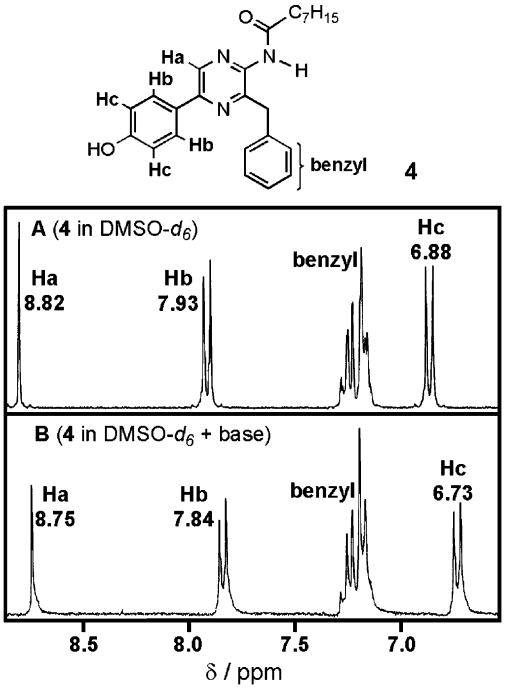

Fig. 9. ^{1}H NMR spectra of **4** (4.2×10^{-3} mol dm^{-3}) in DMSO-d_6 in the absence (A) and presence of 1,1,3,3-tetramethylguanidine (base, 4.2×10^{-3} mol dm^{-3}) (B) at 25 ± 1°C.

To confirm the generation of **4**($\mathbf{O}^-$) in a polar solvent, we analyzed the formation of **4**($\mathbf{O}^-$) in DMSO quantitatively, and investigated ^{1}H and ^{13}C NMR spectra of **4**($\mathbf{O}^-$) in DMSO-d_6. Fig. 8A illustrates absorption spectral changes of **4** in DMSO following the addition of various concentrations of 1,1,3,3-tetramethylguanidine. The absorption peak (λ_{max} 425 nm) of **4**($\mathbf{O}^-$) increased along with decrease of the peak of the neutral form of **4** (λ_{max} 337 nm). The isosbestic point was observed at 344 nm, indicating the quantitative formation of **4**($\mathbf{O}^-$). This spectral change was evaluated by a double reciprocal plot (Fig. 8B), to give the equilibrium constant K for the formation of **4**($\mathbf{O}^-$) from **4** and 1,1,3,3-tetramethylguanidine as $480 \pm 40\,\mathrm{mol^{-1}\,dm^3}$ at 25°C.

^{1}H NMR spectra of **4** in DMSO-d_6 (Fig. 9) show a higher magnetic field shift of the protons of 4-hydroxyphenyl and pyrazine rings of **4** induced by adding 1,1,3,3-tetramethylguanidine, although other protons showed negligible shift. This result is consistent with increase of an anionic character by generation of **4**($\mathbf{O}^-$). ^{13}C NMR spectra of **4** in DMSO-d_6 (Fig. 10) also showed characteristic chemical-shift changes in a low magnetic field region following the addition of 1,1,3,3-tetramethylguanidine. The direction of the chemical-shift changes by generation of **4**($\mathbf{O}^-$) is explained by a difference of electron density between the neutral form of the model structure (**IV**) and its phenolate anion (**V**) as estimated by the AM1 calculation summarized in Table 1. Major changes of the chemical-shift for carbons (Nos. 2, 4, 5, 7, and 11) correlate well with the calculated changes in net atomic charge. These observations confirm the

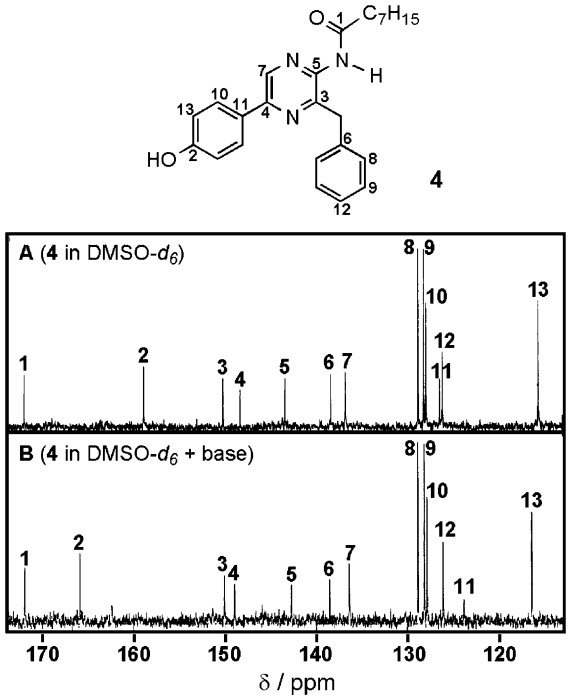

Fig. 10. ^{13}C NMR spectra of **4** ($4.2 \times 10^{-3}\,\mathrm{mol\,dm^{-3}}$) in DMSO-$d_6$ in the absence (A) and presence of 1,1,3,3-tetramethylguanidine (base, $4.2 \times 10^{-3}\,\mathrm{mol\,dm^{-3}}$) (B) at 25 ± 1°C. The assignment of all carbons was established by COSY, HMQC, and HMBC measurements.

Table 1
^{13}C-NMR spectra of **4** in DMSO-d_6 in the absence and presence of 1,1,3,3-tetramethylguanidine, and net atomic charges of model compounds **IV** and **V** calculated by AM1

Carbon No.	Chemical shift δ (ppm)			Net atomic charge		
	4[a]	**4** + base[b]	$\Delta\delta$[c]	**IV**	**V**	Δ(**V**–**IV**)
1	172.2	172.0	−0.2	0.31	0.29	−0.02
2	159.0	165.9	6.9	0.09	0.29	0.20
3	150.4	150.1	−0.3	−0.09	0.03	0.12
4	148.5	149.0	0.5	−0.04	0.11	0.15
5	143.5	142.7	−0.8	0.08	−0.10	−0.18
6	138.4	138.5	0.1	–	–	–
7	136.8	136.4	−0.4	−0.08	−0.17	−0.09
8	128.9	128.8	−0.1	–	–	–
9	128.3	128.1	−0.2	–	–	–
10	128.0	127.8	−0.2	−0.08	−0.02	0.06
11	126.5	123.8	−2.7	−0.07	−0.27	−0.20
12	126.2	126.1	−0.1	–	–	–
13	115.8	116.5	0.7	−0.22	−0.32	−0.10
$-CH_2Ph$	39.0	39.0				
$-C_7H_{15}$	35.4, 31.2	35.3, 31.1				
	28.6, 28.5	28.6, 28.4				
	24.9, 22.1	24.9, 22.0				
	14.0	13.9				

[a] The spectrum of **4** ($4.2 \times 10^{-3}\,\mathrm{mol\,dm^{-3}}$) was observed in DMSO-$d_6$ at 25 ± 1°C.
[b] The spectrum of **4** was measured in DMSO-d_6 containing 1,1,3,3-tetramethylguanidine (base, $4.2 \times 10^{-3}\,\mathrm{mol\,dm^{-3}}$).
[c] $\Delta\delta = \delta(\mathbf{4} + \mathrm{base}) - \delta(\mathbf{4})$.

generation of **4**($\mathbf{O}^-$) in polar solvents. The AM1 result also shows a bond alternation in the phenolate anion (**V**), suggesting the contribution of quinoid structure **VI** in the resonance structures [19].

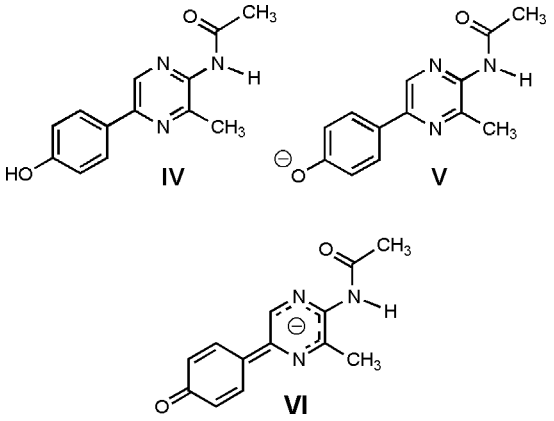

3.3. Spectral shift of phenolate anion fluorescence of **4** dependent upon solvent polarity

Fluorescence of phenolate anion **4**($\mathbf{O}^-$) in benzene and chloroform was observed by electronic excitation of a hydrogen-bonded complex of **4** with *n*-butylamine, and fluorescence of **4**($\mathbf{O}^-$) in polar solvents was observed by electronic excitation of **4**($\mathbf{O}^-$). These results indicate that fluorescence maxima of **4**($\mathbf{O}^-$) shows a bathochromic shift with increase of solvent polarity. Fluorescence maxima in benzene and chloroform were 466 and 502 nm, respectively.

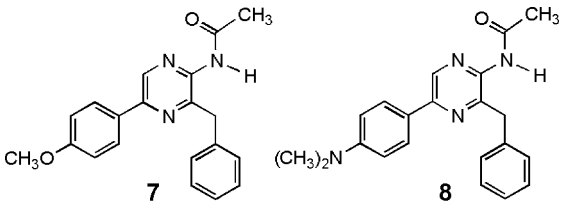

These wavelengths were much shorter than those in DMSO, DMF, and acetonitrile. In order to evaluate the solvent effect on the fluorescence property of **4**($\mathbf{O}^-$), fluorescence emission energies E_F were correlated against the solvent polarity scale $E_T(30)$, which is generally used to evaluate the solvatochromism of electronic transitions with CT character (Fig. 11) [28]. Fig. 11 shows the results observed in the mixed solvents of benzene and chloroform, as well as the reported results of coelenteramide analogues **7** and **8** [20]. The $E_T(30)$ values of the mixed solvents were estimated by measurement of the absorption spectra of 2,6-diphenyl-4-(2,4,6-triphenyl-1-pyridino)phenoxide. The $E_T(30)$ values at 5:1, 2:1, 1:1, 1:2, 1:5, 1:20, and 1:30 mixtures of chloroform and benzene were 38.9, 38.8, 38.4, 38.0, 37.5, 36.4, and 36.2 kcal mol^{-1}, respectively. In these mixed solvents, the E_F values of **4**($\mathbf{O}^-$) observed were 57.0, 57.1, 57.2, 57.9, 58.6, 59.1, and 59.9 kcal mol^{-1}, respectively. The plot for the mixed solvents indicates that the

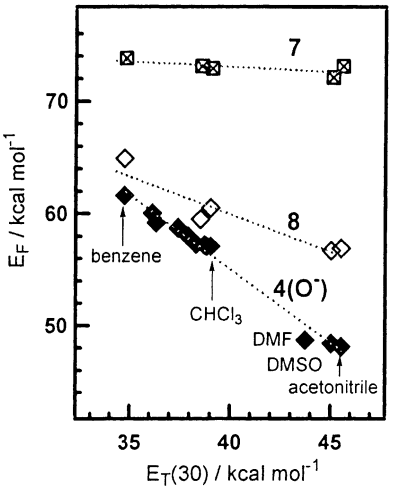

Fig. 11. Plots of fluorescence emission energies E_F for **4**($\mathbf{O}^-$), **7**, and **8** against the solvent polarity parameter $E_T(30)$.

E_F values of **4**($\mathbf{O}^-$) correlate linearly with $E_T(30)$ values. The points for acetonitrile, DMF, and DMSO are found on the line extrapolated from the points of the mixed solvents. This linear relationship for **4**($\mathbf{O}^-$) is similar to that for **7** and **8**, indicating that the singlet-excited state of the phenolate anion has an intramolecular CT character [20]. In the excited state of **4**($\mathbf{O}^-$), a negative charge migrates from the electron-donating 4-oxidophenyl group to the electron-accepting pyrazine ring to give a CT state in a similar manner to other reported electron donor-acceptor compounds such as the 2-(arylamino)naphthalene-6-sulfonate derivatives [29]. The regression line for **4**($\mathbf{O}^-$) is steeper than those for **7** and **8** in the order of **4**($\mathbf{O}^-$) > **8** > **7**. This order corresponds with the electron-donating property of a substituent **D** at the *para* position of the phenyl group at C5. This order also matches the order of the modified Hammett σ_p^+ constants for substituent **D**s; $\mathbf{O}^-$ ($\sigma_p^+ = -2.30$) < $N(CH_3)_2$ ($\sigma_p^+ = -1.70$) < OCH_3 ($\sigma_p^+ = -0.78$) [30]. In the CT excited state of a coelenteramide analogue, the phenyl group at C5 would be positively charged and the pyrazine ring would be negatively charged (Scheme 4). A substituent **D** would regulate the stability of the positively charged phenyl ring at C5 by the resonance effect. Thus, it is reasonable to evaluate the substituent effect of **D** using the σ_p^+ constants, since σ_p^+ constants have previously been used for evaluating substituents of a conjugated system which are able to delocalize a positive charge [31]. From these results, it is established that the singlet-excited

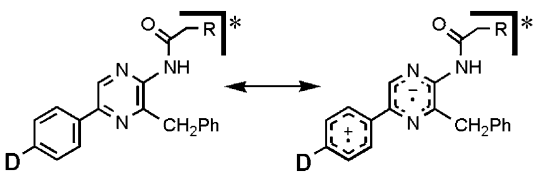

Scheme 4.

states of phenolate anions of coelenteramide derivatives have an intramolecular CT character and show fluorescence spectral changes dependent upon solvent polarity. It is noteworthy that the fluorescence maximum of phenolate anion in benzene is close to the bioluminescence maximum at 465–470 nm.

3.4. Phenolate anion fluorescence of fluorinated coelenteramide analogues **6a–c**

Properties of phenolate anions of fluorinated coelenteramide analogues **6a–c** in benzene were studied in order to evaluate the substituent effect of the fluoro group on the fluorescent property of coelenteramide and the bioluminescent property of fluorinated semi-synthetic AQs [17]. As shown in Fig. 12, formation of 1:1 hydrogen-bonded complexes of fluorinated analogues **6a–c** with *n*-butylamine

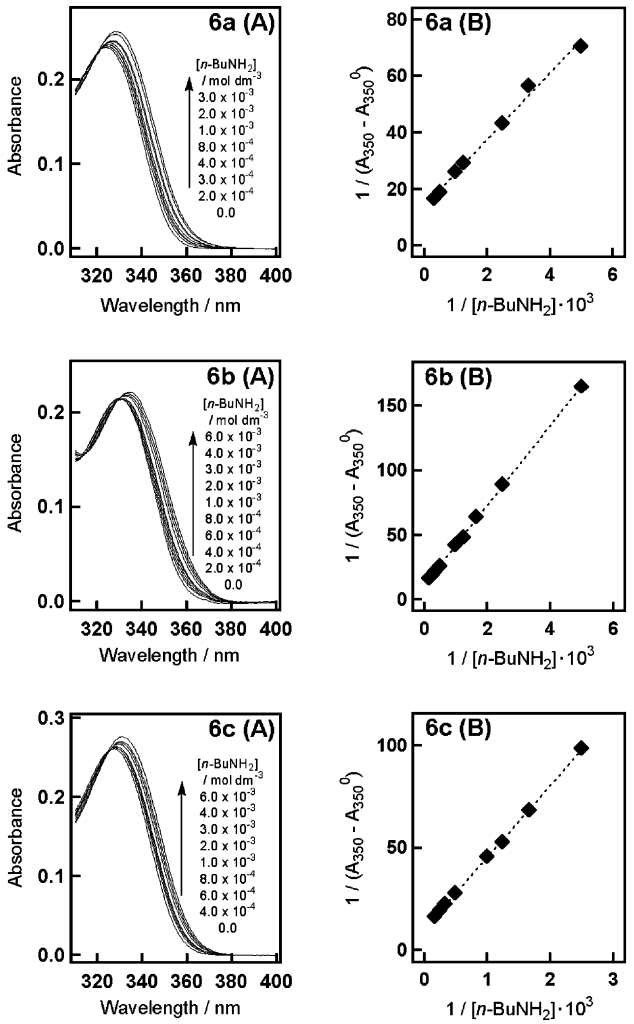

Fig. 12. (A) Absorption spectra of **6a** (1.5×10^{-5} mol dm^{-3}), **6b** (1.5×10^{-5} mol dm^{-3}), and **6c** (1.5×10^{-5} mol dm^{-3}) in benzene containing various concentrations of *n*-butylamine at 25 ± 1°C. (B) Double reciprocal plots of $1/(A_{350} - A_{350}{}^0)$ vs. 1/[*n*-butylamine] for the formation of the hydrogen-bonded complexes of **6a–c** with *n*-butylamine.

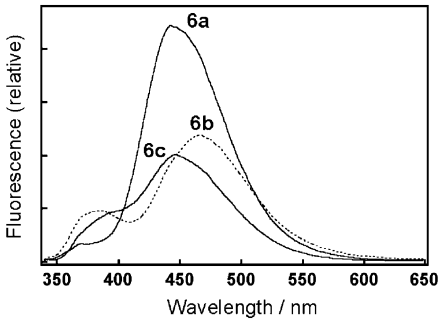

Fig. 13. Fluorescence spectra of **6a–c** (1.5×10^{-5} mol dm^{-3}) in benzene containing *n*-butylamine (0.010 mol dm^{-3}). $\lambda_{ex} = 330$ nm.

was quantitatively evaluated by absorption spectra. Fig. 13 exhibits fluorescence spectra of **6a–c** in benzene in the presence of *n*-butylamine, to show the fluorescence peaks of phenolate anions at 440–466 nm. Fluorescence emission of phenolate anions **6a**($\mathbf{O}^-$)–**6c**($\mathbf{O}^-$) would be caused by electronic excitation of the 1:1 hydrogen-bonded complexes of **6a–c** with *n*-butylamine in the manner similar to that of **4** (Scheme 3). Fluorescence maxima (λ_{max}), quantum yields (ϕ_{FL}), and equilibrium constants (K) for the formation of hydrogen-bonded complexes in benzene are summarized in Table 2 accompanied by those for **4**. Analogues **6a** and **6c** showed blue-shifted emission maxima around 440 nm for the phenolate anions **6a**($\mathbf{O}^-$) and **6c**($\mathbf{O}^-$), although phenolate anion **6b**($\mathbf{O}^-$) fluoresced at the same maximum (λ_{max} 466 nm) as **4**($\mathbf{O}^-$). The fluorescence quantum yields ϕ_{FL} of monofluorinated phenolate anions **6b**($\mathbf{O}^-$) and **6c**($\mathbf{O}^-$) are similar to that of **4**($\mathbf{O}^-$). Difluorinated phenolate anion **6a**($\mathbf{O}^-$) shows a relatively high ϕ_{FL} value. The fluoro-substituent effect is also shown in the increase of *K*. The *K* values increased probably due to increase of acidity of the 4-hydroxyphenyl group by fluoro-substitution [32]. The blue-shifted fluorescence emission of **6a**($\mathbf{O}^-$) and **6c**($\mathbf{O}^-$) originates from the fluoro-substitution at position 2 of the 4-hydroxyphenyl group. As a preliminary calculation, geometries of phenolate anion models **V** and **VIIa–c** were optimized by AM1 to evaluate the fluoro-substituent effect (Scheme 5). The AM1 results (Table 3) indicate that fluoro-substitution moderately lowers energy levels of

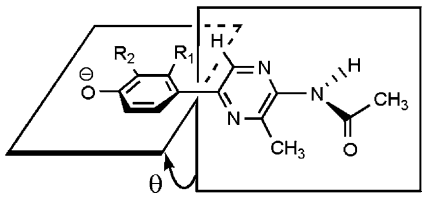

V: $R_1 = R_2 = H$
VIIa: $R_1 = R_2 = F$
VIIb: $R_1 = H$, $R_2 = F$
VIIc: $R_1 = F$, $R_2 = H$

Scheme 5.

Table 2
Spectral properties of coelenteramide analogues **4**, **6a–c**, and their phenolate anions in benzene, and formation constant K of hydrogen-bonded complexes of **4** and **6a–c** with *n*-butylamine in benzene at 25°C

Compound	Neutral form			Phenolate anion[b]		K ($mol^{-1}\,dm^3$)[c]
	λ_{max}(abs)[a] (nm) (ε)	λ_{max}(fl)[a] (nm)	Φ_F	λ_{max}(fl)[a] (nm)	Φ_F	
4	331 (14500)	381	0.24	466	0.2	220 ± 30
6a	324 (15800)	376	0.18	442	0.6	1200 ± 200
6b	330 (14300)	382	0.23	466	0.2	360 ± 15
6c	327 (17400)	380	0.12	440	0.3	301 ± 14

[a] λ_{max}(abs) is the absorption maximum and λ_{max}(fl) is the fluorescence maximum.
[b] Fluorescence spectra of phenolate anions were observed by electronic excitation of hydrogen-bonded complexes of **4** or **6a–c** with *n*-butylamine in benzene ($[n\text{-BuNH}_2] = 4.0 \times 10^{-3}\,mol\,dm^{-3}$, $\lambda_{ex} = 330\,nm$).
[c] K values were estimated by using the absorption spectral changes shown in Figs. 4 and 12.

Table 3
AM1 calculation of phenolate anion models **V** and **VIIa–c** of coelenteramide analogues

Models	Energy level (eV)		Torsion angle θ (°)
	HOMO	LUMO	
V	−3.62	2.77	10
VIIa	−3.92	2.49	28
VIIb	−3.72	2.61	10
VIIc	−3.83	2.65	26

HOMO and LUMO, but do not explain the similarity in fluorescence pattern between **6a**(**O**$^-$) and **6c**(**O**$^-$) and between **4**(**O**$^-$) and **6b**(**O**$^-$). It is noteworthy that the torsion angles θ between the pyrazine ring and the oxidophenyl ring of **VIIa** (28°) and **VIIc** (26°) are similar to each other and are larger than those of **V** (10°) and **VIIb** (10°). This result is consistent with the torsion-angle changes of biphenyl derivatives by fluoro-substitution [33,34]. The fluorine atom of 2-fluorobiphenyl increases the rotational potential about the inter-ring bond as a steric effect. The fluorine atom at position 2 of the 4-oxidophenyl group in **VIIa** and **VIIc** also increases the rotational potential about the inter-ring bond between the pyrazine ring and the oxidophenyl ring. This steric effect of the fluoro-substitution regulates the π-conjugation between the pyrazine ring and the oxidophenyl ring. Thus, fluoro-substitution controls the properties of the singlet-excited states of phenolate anions with intramolecular CT character by a steric effect more than an electronic effect. This explanation would account for the blue-shifted bioluminescence of fluorinated semi-synthetic AQ containing coelenterazine analogues **3a** [17].

3.5. The light-emitter in aequorin bioluminescence

The variation of AQ bioluminescence wavelength in the range 440–480 nm has been observed following chemical modifications of coelenterazine **1** [7,9,10,35], mutations of apoAQ [8], and changes in bioluminescence conditions [36]. This phenomenon may be caused by changes in the interaction between the micro-environment of the active site in apoAQ and the light-emitter. To understand the variable wavelength of light emission in AQ bioluminescence, it is important to note that the fluorescent properties of light-emitters are changeable dependent upon the micro-environment surrounding the excited molecule. Our results confirm that the singlet-excited states of phenolate anions of coelenteramide derivatives have an intramolecular CT character, and that the stabilities of the excited phenolate anions change dependent upon solvent polarity. Solvent molecules create a micro-environment surrounding solute molecules as solvation, although the solvent molecules are not organized as in a protein environment. On the other hand, it has been reported that the fluorescent properties of amide anions of coelenteramide analogues are less sensitive to changes in micro-environment [19,37]. Because of the unstability of amide anions of coelenteramide analogues, however, it has been difficult to investigate their fluorescent properties quantitatively. Only the fluorescence emission wavelengths of amide anions have been reported for several solvents in the presence of strong bases [19,37]. In the solvent polarity range (CH_2Cl_2, diglyme, THF, DMSO, DMF, and acetonitrile), the emission wavelengths of amide anions were variable in the range 450–470 nm. Therefore, the bulk of data on the variability of the emission wavelength from excited phenolate anion **I** supports the variation of bioluminescence wavelength of AQs more from this anion than from amide anion **II**. In apoAQ, a micro-environment created by polypeptide chains at the active site regulates stability of the CT excited state of **I** and thus determining the emission wavelength of AQ bioluminescence.

Under the experimental conditions in this research, we could selectively observe the formation of phenolate anion **4**(**O**$^-$) from **4** as an ionic species, and the formation of an amide anion has never been observed from **4** and **5**. These observations are consistent with a general explanation that phenolate anion **I** is the most stable anionic species generated from **2**. Thus, the evidence reported that the fluorescence spectrum of BFP obtained after a bioluminescence reaction matches the bioluminescence spectrum supports the assignment of ionic structure **I** as the excited

light-emitter in AQ bioluminescence. The fluorescent behavior of BFP also resembles that of *Cypridina* oxyluciferin **9** in the presence of *Cypridina* luciferase. In the *Cypridina* bioluminescence system, the fluorescence spectrum of the complex between **9** and *Cypridina* luciferase also matches the bioluminescence spectrum [38]. It has been proposed that the amide moiety of **9** in the excited state is the N–H form during a bioluminescence reaction [39,40]. Similarly, in the AQ bioluminescence reaction, the amide moiety of **1** most likely changes to the N–H form, and the 4-hydroxyphenyl group at C5 deprotonates to give its anionic form before generating the excited state of **I**.

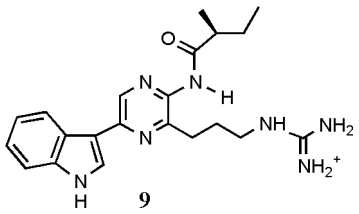

9

Our results also confirm that fluoro-substitution at position 2 on the 4-hydroxyphenyl group at C5 of **2** causes a change of the torsion angle θ between the pyrazine ring and the 4-hydroxyphenyl ring due to steric hindrance. This conformational change gives rise to blue-shifted fluorescence emission from the CT excited state of a phenolate anion. These fluorescent behaviors of the CT excited states of fluorinated coelenteramide derivatives explain the bioluminescent properties of fluorinated semi-synthetic AQs. Therefore, these results again support assignment to phenolate anion **I**. It is noteworthy that the fluorescence maximum of phenolate anion **I** in benzene is close to the bioluminescence maximum at 465–470 nm. This observation helps us to propose the hypothesis that the active site of apoAQ creates a hydrophobic micro-environment similar to the micro-environment of benzene-solvation. The crystal structure of AQ also supports this hypothesis. In the supramolecular structure of AQ [5], oxygenated coelenterazine is located in the hydrophobic active site which mainly consists of the aromatic amino acid residues tyrosine and tryptophan along with histidine and leucine residues. This hydrophobic active site of apoAQ may regulate the character of the excited phenolate anion **I** in a manner similar to benzene-solvation. In AQ, the oxygenated coelenterazine is also fixed by the hydrogen-bonding network [5]. Specifically, the hydrogen-bonding interaction around the 4-hydroxyphenyl group at position 6 of **1** may assist in the formation of phenolate anion **I** during the bioluminescence reaction of AQ. A crystal structure analysis of BFP will further elucidate this.

4. Concluding remarks

A method to observe the fluorescence of phenolate anion **4**($\mathbf{O}^-$) in non-polar solvents was established by electronic excitation of a 1:1 hydrogen-bonded complex of **4** with an HBD molecule such as *n*-butylamine. In polar solvents, the fluorescent properties of **4**($\mathbf{O}^-$) directly generated using base 1,1,3,3-tetramethylguanidine were clarified. These results confirm that the singlet-excited state of phenolate anion **I** of coelenteramide **2** has an intramolecular CT character, and its fluorescence emission wavelength is changeable dependent upon solvent polarity. We also confirm the substituent effect of a fluoro group in the 4-oxidophenyl group at C5 of **4**($\mathbf{O}^-$). The fluoro-substitution at position 2 on the 4-oxidophenyl group increases steric hindrance and decreases π-conjugation between the 4-oxidophenyl group and the pyrazine ring, yielding a blue-shifted fluorescence. These results consistently support the assignment of phenolate anion **I** as the ionic structure of the excited light-emitter in BFP during AQ bioluminescence. In a bioluminescence reaction of AQ, interactions between the excited light-emitter and a polypeptide micro-environment of apoAQ determine the emission wavelength bioluminescence by controlling the stability of the CT excited state of **I**.

Acknowledgements

This work was supported by a grant from the Ministry of Education, Science, Sports, and Culture of Japan [No. 11640578]. We thank Dr. H. Ikeda and Professor T. Miyashi (Tohoku University) for kind discussions and for carrying out measurements of mass spectra and elemental analysis.

References

[1] O. Shimomura, F.H. Johnson, Y. Saiga, J. Cell. Comp. Physiol. 59 (1962) 223.
[2] F.H. Johnson, O. Shimomura, Meth. Enzymol. 57 (1978) 271.
[3] Y. Ohmiya, T. Hirano, Chem. Biol. 3 (1996) 337.
[4] W.T. Mason, Fluorescent and Luminescent Probes for Biological Activity, 2nd Edition, Academic Press, London, 1999.
[5] J.H. Head, S. Inouye, K. Teranishi, O. Shimomura, Nature 405 (2000) 372.
[6] O. Shimomura, F.H. Johnson, Tetrahedron Lett. (1973) 2963.
[7] O. Shimomura, B. Musicki, Y. Kishi, Biochem. J. 261 (1989) 913.
[8] Y. Ohmiya, M. Ohashi, F.I. Tsuji, FEBS Lett. 301 (1992) 197.
[9] O. Shimomura, B. Musicki, Y. Kishi, Biochem. J. 251 (1988) 405.
[10] O. Shimomura, S. Inouye, B. Musicki, Y. Kishi, Biochem. J. 270 (1990) 309.
[11] F. McCapra, Y.C. Chang, J. Chem. Soc., Chem. Commun. (1967) 1011.
[12] T. Goto, S. Inoue, S. Sugiura, K. Nishikawa, M. Isobe, Y. Abe, Tetrahedron Lett. (1968) 4035.
[13] O. Shimomura, F.H. Johnson, Nature 227 (1970) 1356.
[14] J. March, Advanced Organic Chemistry, 4th Edition, Wiley, New York, 1992.
[15] N.J. Turro, Modern Molecular Photochemistry, University Science Book, Sausalito, 1991.
[16] T. Hirano, I. Mizoguchi, M. Yamaguchi, F.Q. Chen, M. Ohashi, Y. Ohmiya, F.I. Tsuji, J. Chem. Soc., Chem. Commun. (1994) 165.
[17] T. Hirano, Y. Ohmiya, S. Maki, H. Niwa, M. Ohashi, Tetrahedron Lett. 39 (1998) 5541.

[18] T. Hirano, Y. Gomi, T. Takahashi, K. Kitahara, F.Q. Chen, I. Mizoguchi, S. Kyushin, M. Ohashi, Tetrahedron Lett. 33 (1992) 5771.
[19] O. Shimomura, K. Teranishi, Luminescence 15 (2000) 51.
[20] R. Saito, T. Hirano, H. Niwa, M. Ohashi, J. Chem. Soc., Perkin Trans. 2 (1997) 1711.
[21] M.J.S. Dewar, E.G. Zoebisch, E.F. Healy, J.J.P. Stewart, J. Am. Chem. Soc. 107 (1985) 3902.
[22] Y. Kishi, H. Tanino, T. Goto, Tetrahedron Lett. (1972) 2747.
[23] A. Matsuzaki, S. Nagakura, K. Yoshihara, Bull. Chem. Soc. Jpn. 47 (1974) 1152.
[24] L.M. Tolbert, S.M. Nesselroth, J. Phys. Chem. 95 (1991) 10331.
[25] K.J. Willis, A.G. Szabo, J. Phys. Chem. 95 (1991) 1585.
[26] H.J. Schneider, A.K. Yatsimirsky, Principles and Methods in Supramolecular Chemistry, Wiley, Chichester, UK, 1999.
[27] I.M. Kolthoff, M.K. Chantooni Jr., S. Bhowmik, J. Am. Chem. Soc. 90 (1968) 23.
[28] C. Reichardt, Solvents and Solvent Effects in Organic Chemistry, 2nd Edition, VCH, Weinheim, 1990.
[29] K.M. Kosower, H. Dodiuk, K. Tanizawa, M. Ottolenghi, N. Orbach, J. Am. Chem. Soc. 97 (1975) 2167.
[30] C. Hansch, A. Leo, R.W. Taft, Chem. Rev. 91 (1991) 165.
[31] H.C. Brown, Y. Okamoto, J. Am. Chem. Soc. 80 (1958) 4979.
[32] H. Ratajczak, J. Phys. Chem. 76 (1972) 3000.
[33] E. Ciampi, M.I.C. Furby, L. Brennan, J.W. Emsley, A. Lesage, L. Emsley, Liq. Cryst. 26 (1999) 109.
[34] S. Ando, T. Hironaka, H. Kurosu, I. Ando, Magn. Reson. Chem. 38 (2000) 241.
[35] T. Hirano, R. Negishi, M. Yamaguchi, F.Q. Chen, Y. Ohmiya, F.I. Tsuji, M. Ohashi, Tetrahedron 53 (1997) 12903.
[36] O. Shimomura, Biochem. J. 306 (1995) 537.
[37] K. Teranishi, M. Hisamitsu, T. Yamada, Tetrahedron Lett. 38 (1997) 2689.
[38] O. Shimomura, F.H. Johnson, T. Masugi, Science 164 (1969) 1299.
[39] T. Goto, Pure Appl. Chem. 17 (1968) 421.
[40] T. Goto, H. Fukatsu, Tetrahedron Lett. (1969) 4299.